Selective preconcentrative separation of Hg(II) and Cd(II) by using recycled aluminum adsorbents from water, fish muscles, and cucumber samples

A. B. Abdallah*[a], Ehab A. Abdelrahman [b], Adel M. Youins [a], Wesam A. Ibrahim [a],

Magdi E. Khalifa[a]

[a] Department of Chemistry, Faculty of Science, Mansoura University, El-Gomhoria Street, Mansoura-35516, Egypt

[b] Chemistry Department, Faculty of Science, Benha University, Benha 13518, Egypt

*E-mail: ahmed.bahgat@mans.edu.eg

Figure caption

Fig. S1. The XRD pattern of the BAA (A), IAA (B), and CAA (C).

Fig. S2. Thermal analysis curves (TGA, DTG) of: (A) Cd-BAA, (B) Hg-BAA, (C) Cd-CAA, (D) Hg-CAA, (E) Cd-IAA and (F) Hg-IAA complexes respectively.

Fig. S3. XPS spectra of Al 2p, C1s, N 1s, O 1s, Si 2p, Cd 3d, and Hg 4f for the synthesized BAA sorbent before and after adsorption of mercury and cadmium.

Fig. S4. MEP maps of (a) dibenzoylmethane, (b) isatoic and (c) 5-(chloroacetamide)-2-hydroxybenzoic acid ligands respectively.

Fig. S5. Effect of kinetic on the extraction of Hg(II) and Cd(II) via pseudo first and second order models.

Fig. S6. Freundlich and Langmiur isotherms for the adsorption of Hg(II), and Cd(II) on the surface of BAA, IAA, and CAA.

Table Caption

Table S1. pseudo first and second order parameters for the extraction of Hg(II), and Cd(II) on the surface of different adsorbents.

Table S2. Extraction efficiency by different washing solvents.

Table. S3. Thermodynamic parameters of the extraction of Hg(II) and Cd(II) on the surface of BAA, IAA, and CAA.

Table S4. Langmuir and Freundlich constants of Hg(II) and Cd(II) adsorption.

Table S5. The impact of interference ions on the extraction efficiency of Hg(II) and Cd(II).
Table S6. Analytical figures of merit of the preconcentration procedure.
Table S7. The extraction percentage of mercury and cadmium by different sorbents after different cycles.
Table S8. Comparison of the proposed sorbents (BAA, IAA, and CAA) with the previously reported adsorbents for Hg(II), and Cd(II) detection.

Figures

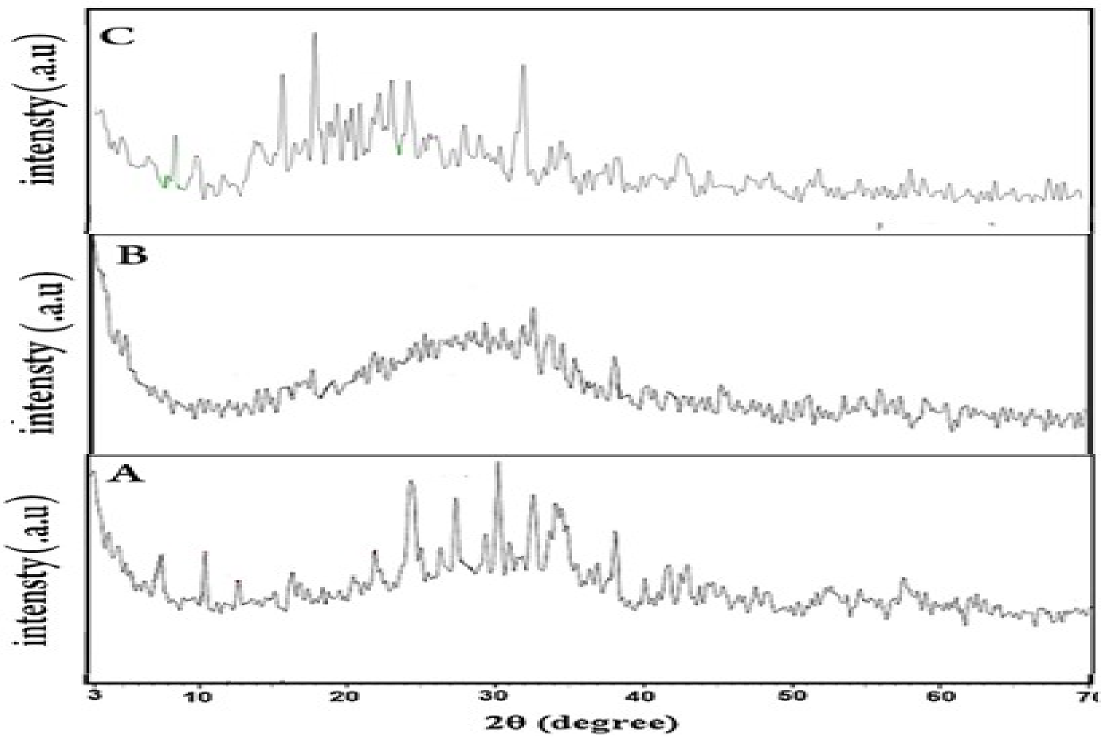

Fig. S1.

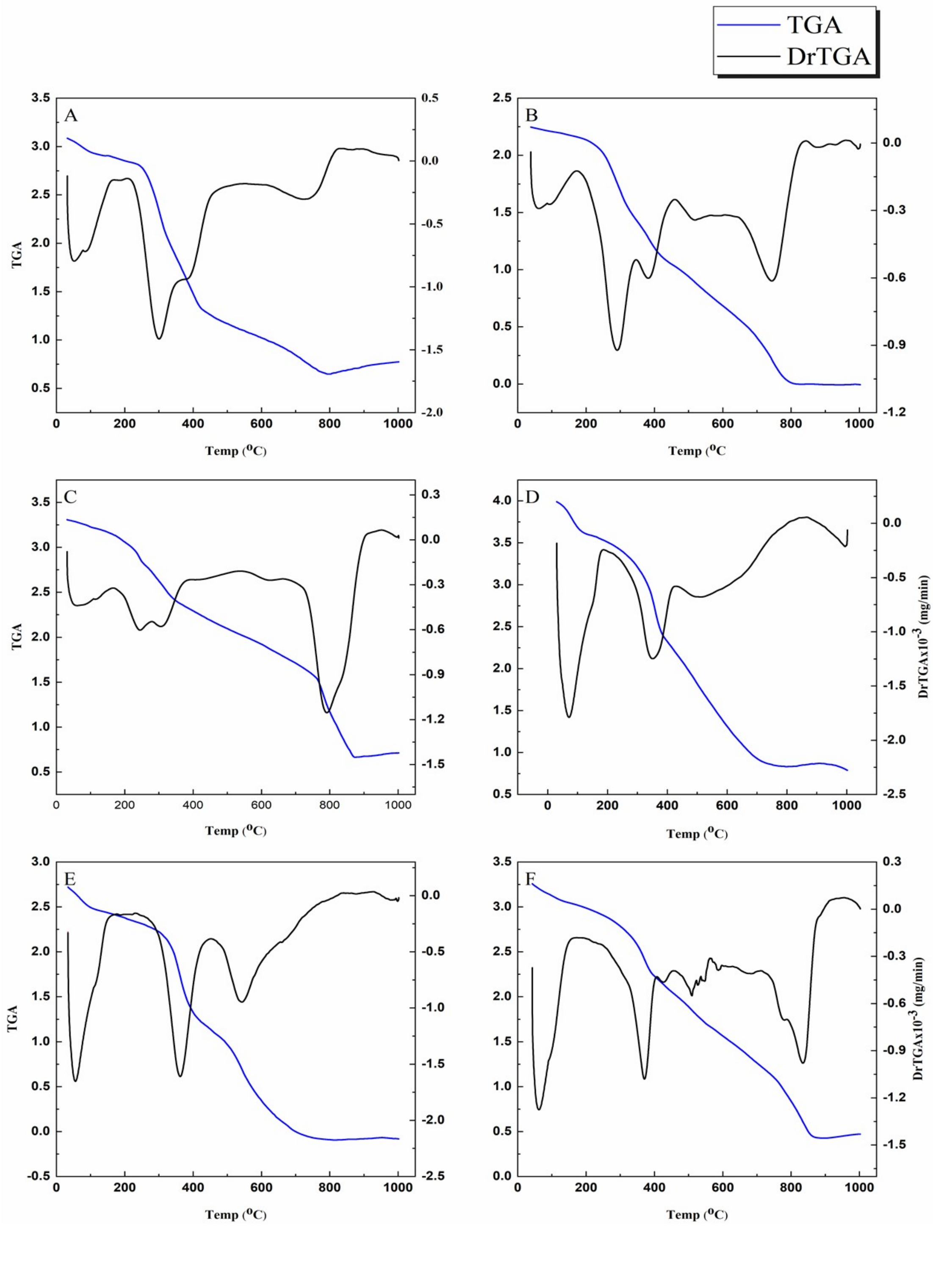

Fig. S2

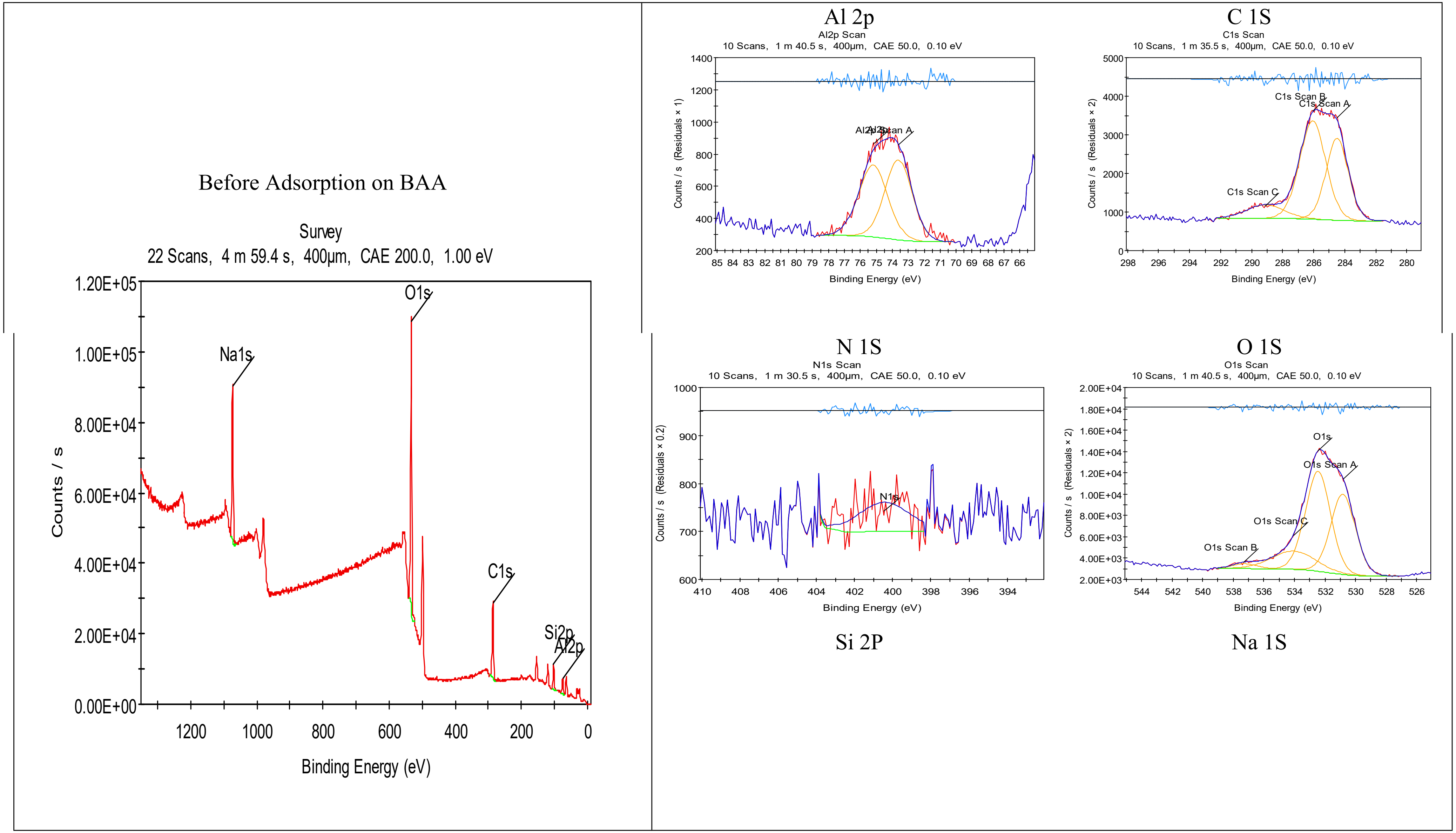
Before Adsorption on BAA
Survey
22 Scans, 4 m 59.4 s, 400µm, CAE 200.0, 1.00 eV
Counts / s
Binding Energy (eV)
Na1s
O1s
C1s
Si2p
Al2p
Al 2p
Al2p Scan
10 Scans, 1 m 40.5 s, 400µm, CAE 50.0, 0.10 eV
Counts / s (Residuals × 1)
Al2p Scan A
C 1S
C1s Scan
10 Scans, 1 m 35.5 s, 400µm, CAE 50.0, 0.10 eV
Counts / s (Residuals × 2)
C1s Scan B
C1s Scan A
C1s Scan C
N 1S
N1s Scan
10 Scans, 1 m 30.5 s, 400µm, CAE 50.0, 0.10 eV
Counts / s (Residuals × 0.2)
N1s
O 1S
O1s Scan
10 Scans, 1 m 40.5 s, 400µm, CAE 50.0, 0.10 eV
Counts / s (Residuals × 2)
O1s
O1s Scan A
O1s Scan C
O1s Scan B
Si 2P
Na 1S

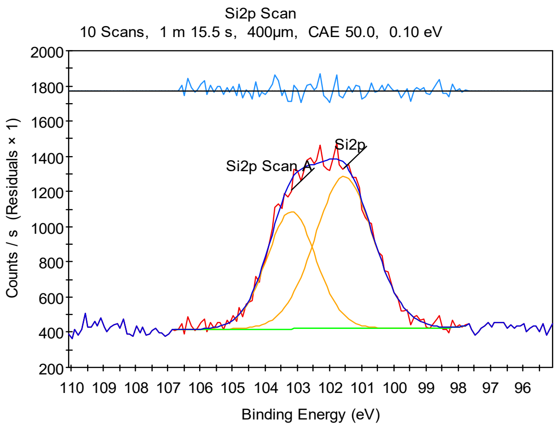

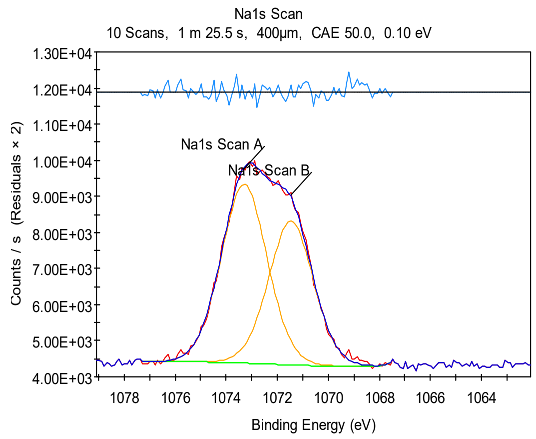

After Hg (II) adsorption on BAA

Al 2p

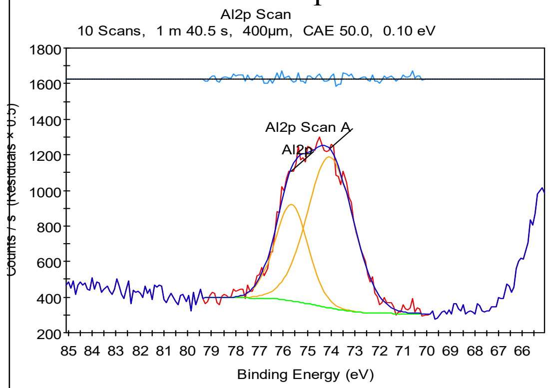

C 1s

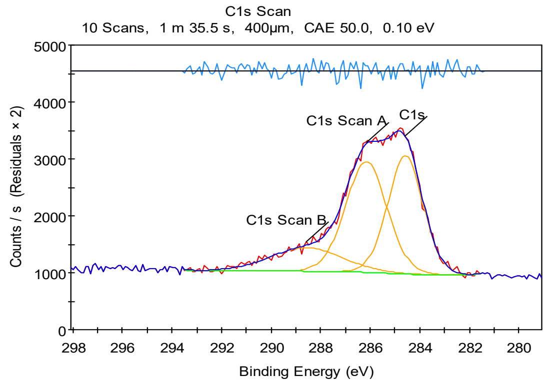

N 1s

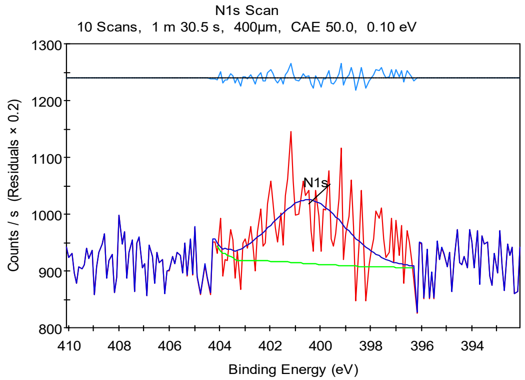

O 1s

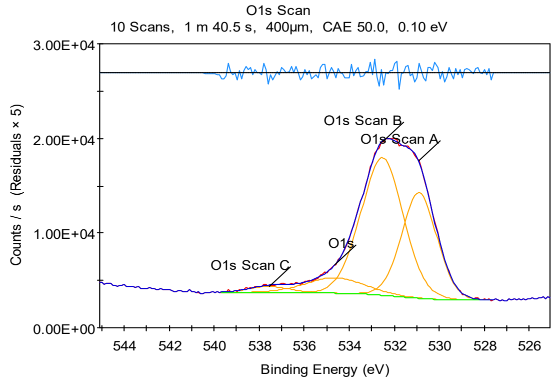

Hg 4f+Si 2p

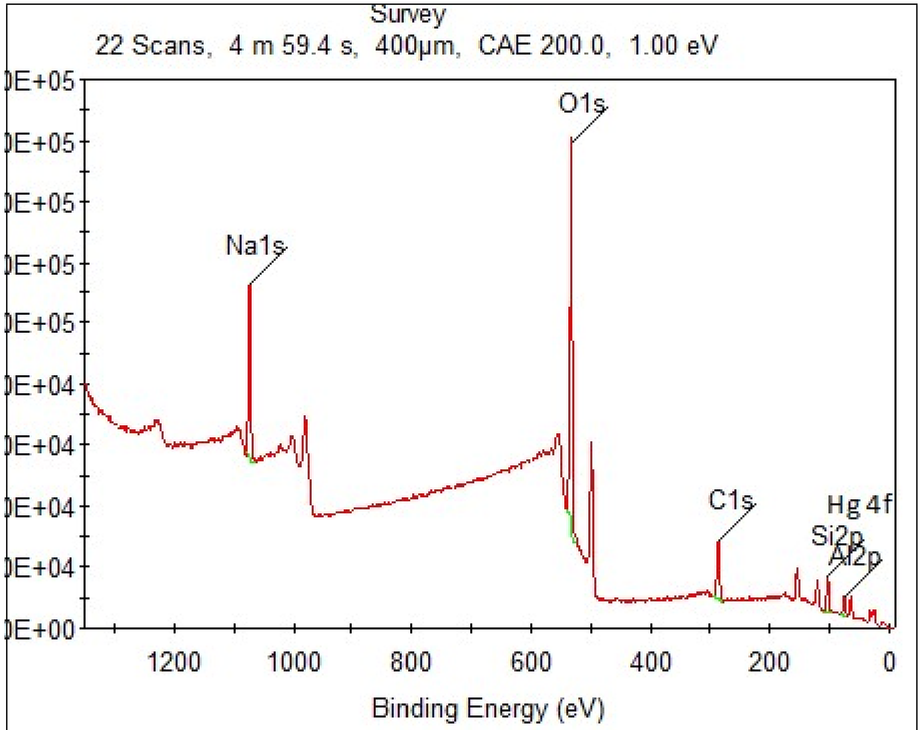

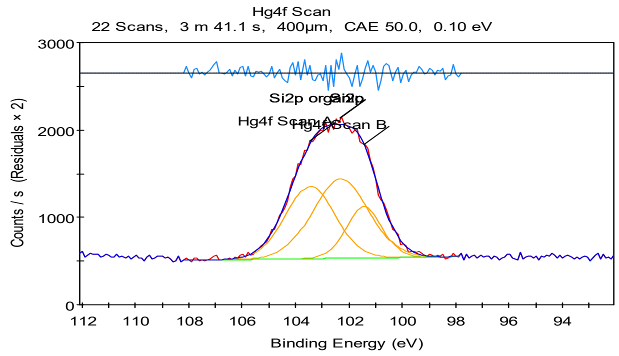

Al 2p

C 1s

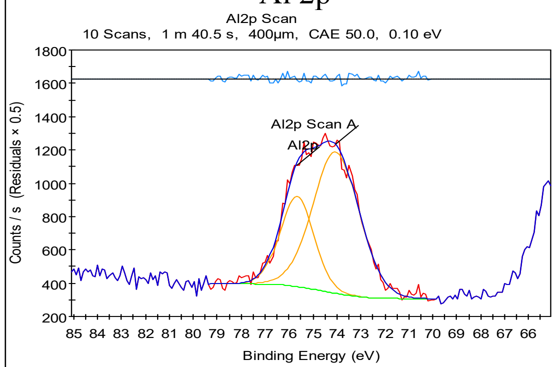

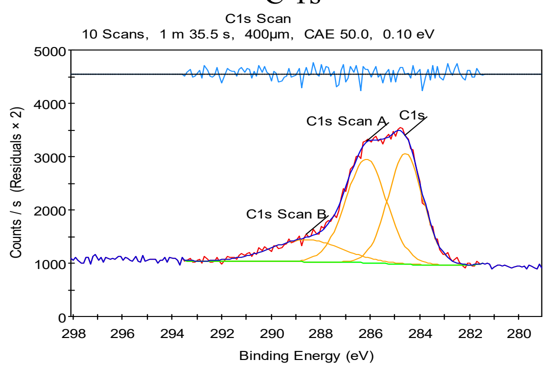

After Cd (II) adsorption on BAA

N 1s

O 1s

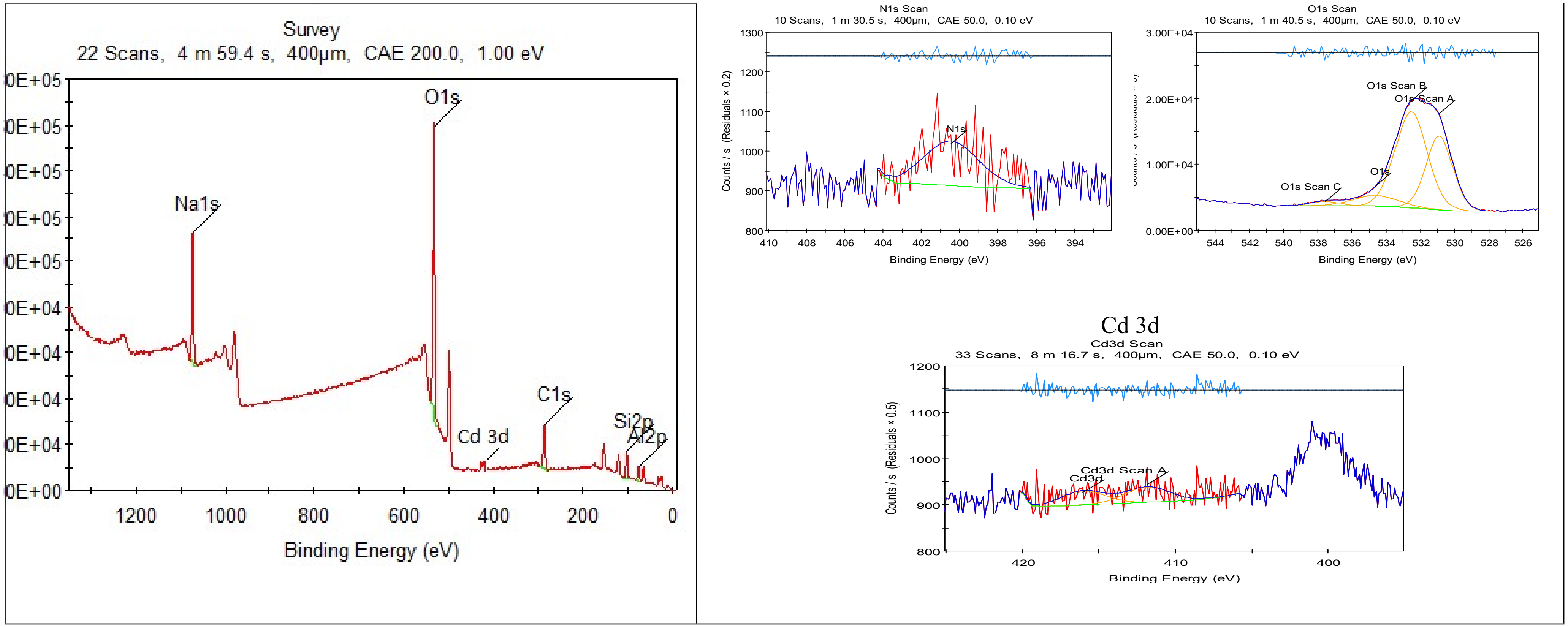

Survey
22 Scans, 4 m 59.4 s, 400µm, CAE 200.0, 1.00 eV
O1s
Na1s
C1s
Cd 3d
Si2p
Al2p
Binding Energy (eV)
N1s Scan
10 Scans, 1 m 30.5 s, 400µm, CAE 50.0, 0.10 eV
N1s
Counts / s (Residuals × 0.2)
Binding Energy (eV)
O1s Scan
10 Scans, 1 m 40.5 s, 400µm, CAE 50.0, 0.10 eV
O1s Scan B
O1s Scan A
O1s
O1s Scan C
Binding Energy (eV)
Cd 3d
Cd3d Scan
33 Scans, 8 m 16.7 s, 400µm, CAE 50.0, 0.10 eV
Cd3d Scan A
Cd3d
Counts / s (Residuals × 0.5)
Binding Energy (eV)

Fig. S3.

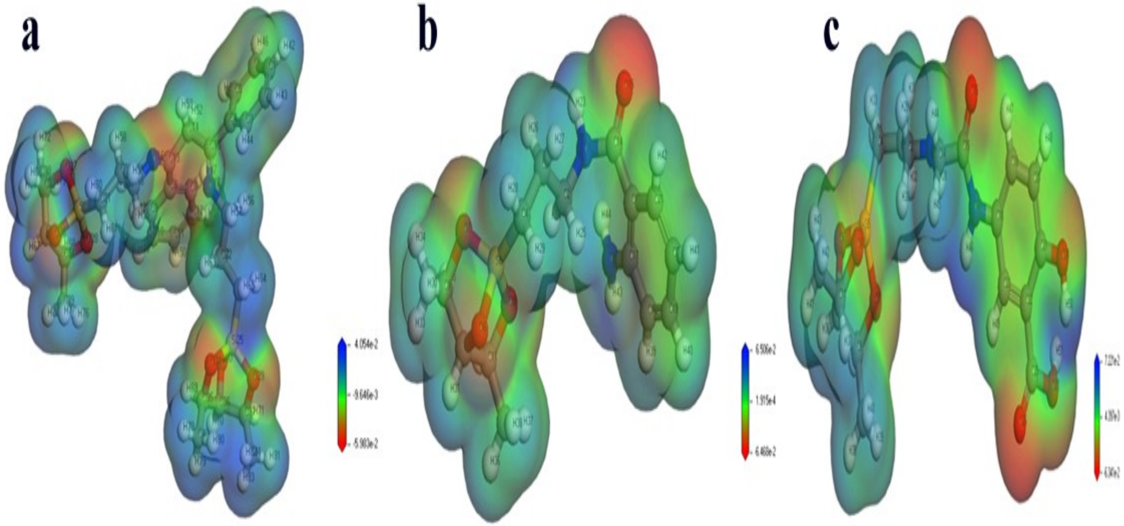
a
b
c

Fig. S4.

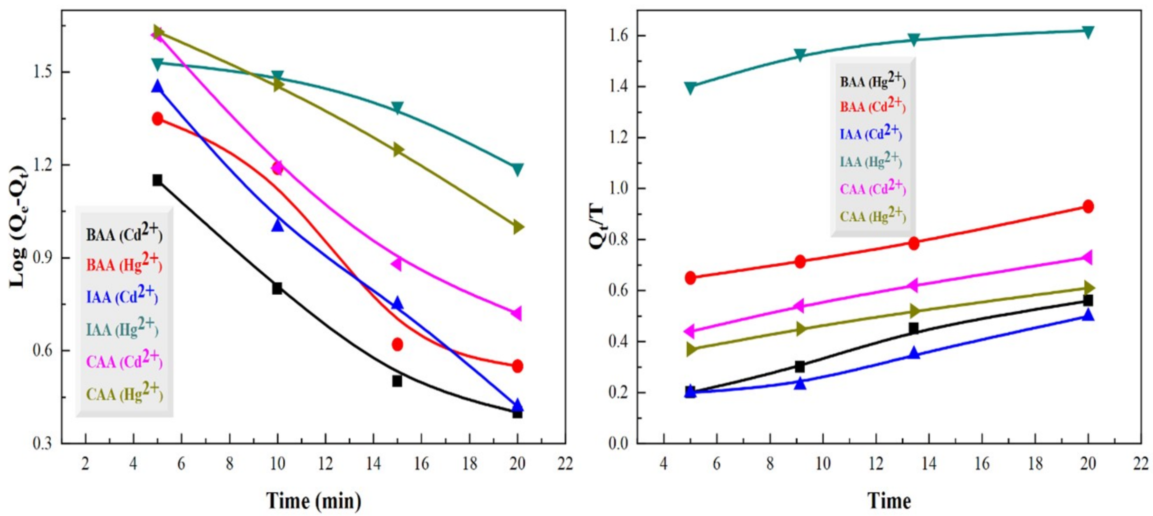
Log (Q_e-Q_t)
Time (min)
BAA (Cd^{2+})
BAA (Hg^{2+})
IAA (Cd^{2+})
IAA (Hg^{2+})
CAA (Cd^{2+})
CAA (Hg^{2+})
Q_t/T
Time
BAA (Hg^{2+})
BAA (Cd^{2+})
IAA (Cd^{2+})
IAA (Hg^{2+})
CAA (Cd^{2+})
CAA (Hg^{2+})

Fig. S5.

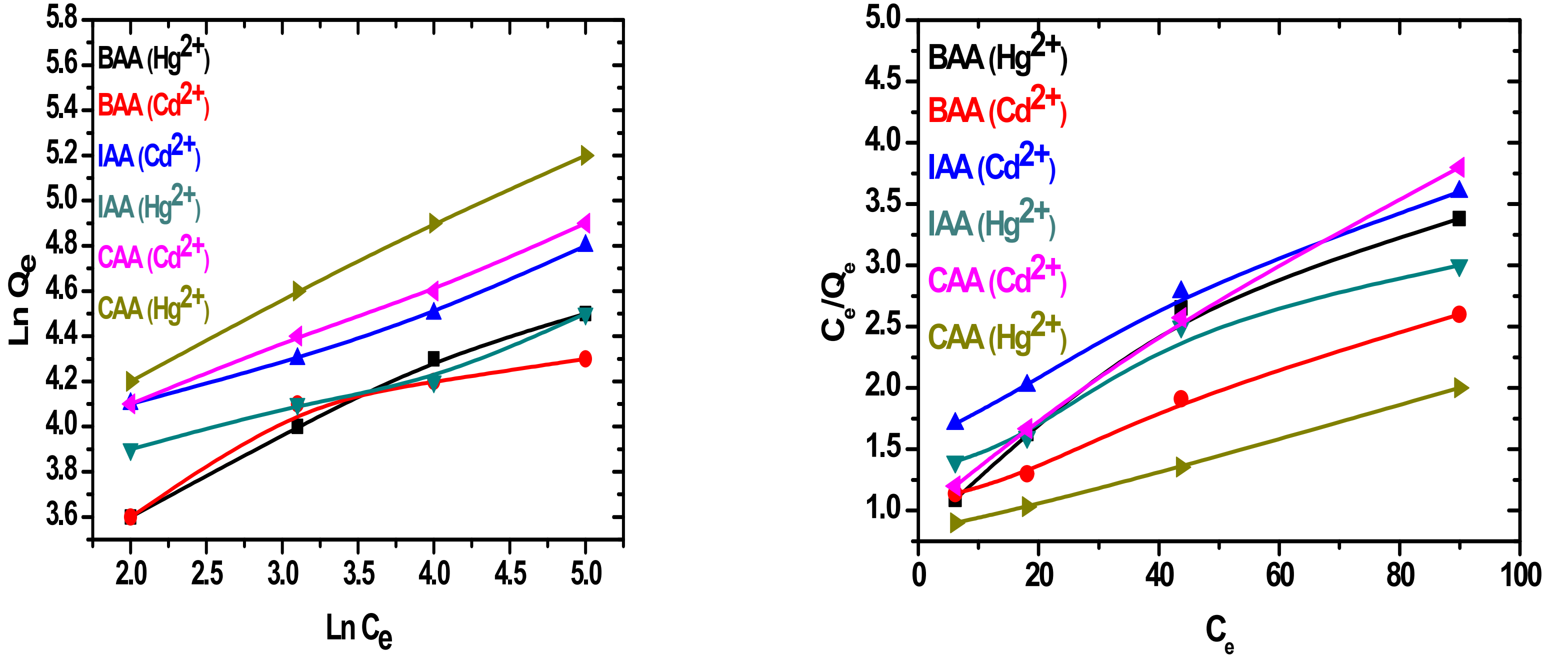

Ln Qe
Ln Ce
BAA (Hg2+)
BAA (Cd2+)
IAA (Cd2+)
IAA (Hg2+)
CAA (Cd2+)
CAA (Hg2+)
Ce/Qe
Ce

Fig. S6.

Tables

Table S1.

Metal	Supporting material	First order model			Second order model		
		K_1 (min^{-1})	Q_{e1} ($mg\ g^{-1}$)	R^2	K_2 ($g\ mg^{-1}\ min^{-1}$)	Q_{e2} ($mg\ g^{-1}$)	R^2
Cd(II)	BAA	0.1154	23.323	0.980	0.00978	39.777	0.994
	IAA	0.1455	50.769	0.956	0.01476	42.7167	0.964
	CAA	0.1426	84.732	0.944	0.01532	50.2512	0.961
Hg(II)	BAA	0.1400	44.565	0.967	0.01040	12.658	0.991
	IAA	0.1075	45.814	0.973	$3.814\ x10^{-3}$	84.745	0.998
	CAA	0.1107	80.7235	0.982	$1.0036\ x10^{-3}$	77.519	0.999

Table S2.

Metal	sorbent	Extraction %							
		HNO_3 (0.1M)	HNO_3 (0.5M)	HCl (0.1M)	HCl (0.5M)	EDTA (0.1M)	EDTA (0.5M)	NaOH (0.1M)	NaOH (0.5M)
Cd(II)	BAA	97.64	95.24	94.67	91.34	95.34	90.17	88.2	90.5
	IAA	97.34	95.31	95.79	91.34	96.37	92.46	86.3	91.2
	CAA	95.14	91.64	93.64	88.97	96.31	90.14	88.7	89.4
Hg(II)	BAA	98.24	96.34	97.60	92.31	96.04	92.34	84.6	91.8

	IAA	96.34	91.37	94.35	91.34	93.47	88.24	89.1	92.1
	CAA	97.56	93.24	94.80	90.42	92.75	87.91	89.4	90.8

Table. S3.

Metal	**Sorbent**	**-ΔG°$_{ads}$ (KJ mol^{-1})**						**ΔH°$_{ads}$ (KJ mol^{-1})**	**ΔS°$_{ads}$ (KJ mol^{-1} k^{-1})**
	Temp (K)	**298**	**303**	**308**	**313**	**318**	**323**		
Cd (II)	**BAA**	-140.21	141.3	-142.4	-143.5	-144.7	-145.8	-73.068	0.225
	IAA	-151.57	-152.79	-154	-155.22	-156.43	-157.65	-79.136	0.243
	CAA	-157.59	-158.85	-160.11	-161.37	-162.63	-163.89	-82.489	0.252
Hg(II)	**BAA**	-151.24	-152.5	-153.7	-155.8	-156.3	-157.6	-74.95	0.256
	IAA	-171.06	-172.48	-173.9	-175.32	-176.74	-178.16	-86.441	0.283
	CAA	-164.61	-165.9	-167.3	-168.68	-170. 3	-171.39	-83.874	0.270

Table S4.

Metal	Sorbents	Langmuir constants			Freundlich constants		
		Qm (mg g^{-1})	K_{Lang} (L mg^{-1})	R^2	Qm (mg g^{-1})	K_{Fre} (mg g^{-1}) (L mg^{-1})$^{1/n}$	R^2
Cd(II)	BAA	60.240	0.0104	0.991	71.265	21.791	0.984
	IAA	62.893	0.0124	0.970	105.61	33.414	0.961
	CAA	62.150	0.0162	0.991	111.04	40.690	0.975
Hg(II)	BAA	101.01	0.00722	0.982	216.668	53.677	0.956
	IAA	101.83	0.0103	0.967	109.30	19.707	0.962
	CAA	175.13	0.00812	0.968	159.11	32.040	0.931

Table S5.

interfering metal ion		Recovery (%)					
		BAA		IAA		CAA	
Type	Concentration (mg L^{-1})	Cd(II)	Hg(II)	Cd(II)	Hg(II)	Cd(II)	Hg(II)
Co(II)	0	98.8	99.1	98.9	98.49	99.87	97.9
	50	97.1	96.4	94.16	98.42	99.56	97.85
	80	97.3	95.3	93.14	95.32	90.24	94.36
	100	96	97.1	93.57	93.61	92.55	96.52
Ni(II)	0	99.2	98.3	98.27	98.35	99.85	98.9
	50	97.9	96.9	94.11	98.32	99.11	97.87
	80	96.7	95.6	97.77	94.32	97.77	96.37
	100	95.3	96.1	90.12	96.16	95.92	93.36
Fe(III)	0	98.7	98.4	97.24	98.57	99.84	99.9
	50	97.6	96.8	94.78	92.28	97.66	96.86
	80	95.9	94.8	93.02	91.34	98.32	93.36
	100	96.2	97.2	92.2	92.6	96.25	96.16
Zn(II)	0	99.3	98.8	98.18	98.49	99.81	98.8
	50	98.4	96.9	97.45	94.19	94.65	96.29
	80	97.1	97.1	95.48	99.53	93.88	96.59
	100	96.2	94.8	93.50	91.52	95.70	94.32
AL(III)	0	99.3	97.9	99.25	98.52	99.87	98.9
	50	98.4	96.4	98.14	98.25	99.81	96.84
	80	97.6	94.8	97.05	95.57	98.05	97.75
	100	96	93.8	96.65	94.89	92.47	96.57

Table S6.

Parameters		Optimum value
Concentration range		**50-300 mg L^{-1}**
LOD	BAA	1.1 mg L^{-1} (Hg(II))
		1.9 mg L^{-1} (Cd(II))
	IAA	9.1 mg L^{-1} (Hg(II))
		10.3 mg L^{-1} (Cd(II))
	CAA	10.6 mg L^{-1} (Hg(II))
		11.2 mg L^{-1} (Cd(II))
LOQ	BAA	3.66 mg L^{-1} (Hg(II))
		6.3 mg L^{-1} (Cd(II))
	IAA	30.33 mg L^{-1} (Hg(II))
		34.3 mg L^{-1} (Cd(II))
	CAA	35.3 mg L^{-1} (Hg(II))
		37.3 mg L^{-1} (Cd(II))
Reusability	BAA	9 times
	IAA	8 times
	CAA	5 times
R^2	BAA	0.99
	IAA	0.95

	CAA	0.96
Adsorption capacity	BAA	234.56 mg g^{-1} (Hg(II)) 229.38 mg g^{-1} (Cd(II))
	IAA	189.72 mg g^{-1} (Hg(II)) 166.43 mg g^{-1} (Cd(II))
	CAA	195.64 mg g^{-1} (Hg(II)) 135.28 mg g^{-1} (Cd(II))

Table. S7.

No. of cycle	Extraction of Hg(II) %			Extraction of Cd(II) %		
	BAA	IAA	CAA	BAA	IAA	CAA
1	98.9	97.8	95.4	96.7	99.1	95.3
2	98.1	96.5	94.8	96.1	98.8	95.1
3	97.9	95.4	94.5	95.6	98.5	94.7
4	97.9	94.6	94.3	94.9	98.5	94.5
5	97.5	94.5	94.2	94.4	98.3	94.3

Table S8.

Metal ion	Adsorbent	Adsorption capacity (mg g^{-1})	Refs.
Cd(II)	Iron oxide (Fe_2O_3)	86.7	(Yu et al., 2021)
Cd(II)	zeolite-supported microscale zero-valent iron (Z-mZVI) w	63.14	(Kong et al., 2017)
Cd(II)	Fe_3O_4/cyclodextrin polymer nanocomposites	27.7	(Badruddoza et al., 2013)
Cd(II)	Activated sepiolite	21.28	(Zhou et al., 2022)
Cd(II)	BAA, IAA, and CAA	229.38, 166.43 and 135.28	This study
Hg(II)	Nano silica Saccharomyces cerevisiae bio-hybrid material	185	(Shukla et al., 2020)
Hg(II)	Modified multiwall carbon nanotubes	174.3	(Esmaeili et al., 2020)
Hg(II)	Ag supported on nanomesoporous silica	151	(Ganzagh et al., 2016)
Hg(II)	mesoporous ZSM-5	172.6	(Abbas et al., 2018)
Hg(II)	BAA, IAA, and CAA	234.56, 189.72 and 195.64	This study